Research Article | Vol. 27, No. 25 / 9 December 2019 / Optics Express 36903
Optics EXPRESS

Ferroelectric liquid crystal mediated fast switchable orbital angular momentum of light

Yuan Liu,[1] Peng Chen,[1,4] Rui Yuan,[1] Chao-Qun Ma,[1] Qi Guo,[2,5] Wei Duan,[1,2] Vladimir G. Chigrinov,[3] Wei Hu,[1] and Yan-Qing Lu[1]

[1]*National Laboratory of Solid State Microstructures, Key Laboratory of Intelligent Optical Sensing and Manipulation, College of Engineering and Applied Sciences, and Collaborative Innovation Center of Advanced Microstructures, Nanjing University, Nanjing 210093, China*
[2]*School of Instrumentation and Optoelectronic Engineering, Beihang University, Beijing 100191, China*
[3]*School of Physics and Optoelectronics Engineering, Foshan University, Foshan 528000, China*
[4]*chenpeng@nju.edu.cn*
[5]*qguo@buaa.edu.cn*

Abstract: Orbital angular momentum (OAM) of light has been extensively studied during the past two decades. Till now, it is a formidable challenge to dynamically manipulate OAM in fast switching speed, good beam quality and low power consumption. Here, an alternative strategy is proposed through the combination of the uniformly-aligned ferroelectric liquid crystal (FLC) and the space-variant photo-patterned nematic liquid crystal. Owing to the excellent electro-optical properties of the adopted FLC, the high-performance electrical switching of OAM, especially, its helicity and the superposed state (*i.e.*, the cylindrical vector beam), can be realized in good quality and high efficiency. The symmetric switching time is down to 120 μs even at a very low driving voltage of 1.7 V/μm. This supplies a practical and universal method towards high-frequency manipulation of OAM and other structured beams.

1. Introduction

Optical vortex (OV), which is characterized by a helical phase-front, carries intrinsic quantized orbital angular momentum (OAM) of light [1,2]. The central phase singularity of its screw-type phase distribution results in a doughnut shape of the transverse intensity profile. OAM adds a brand new degree of freedom to the control of light and has attracted great interests in numerous areas, such as optical tweezers [3,4], classical and quantum communications [5,6], laser processing [7,8], and even astronomic observation [9,10]. Recently, another singular beam, cylindrical vector beam (CVB), has also been investigated with various similar properties [11]. It has spatially variant polarization states and a polarization singularity at the beam center. Actually, CVB and OV are closely related, and can be generalized and geometrically described by the higher-order Poincaré sphere [12,13], whose north/south pole indicates right/left circularly polarized OV with opposite OAM helicity (*i.e.*, eigenstates). CVB can be considered as the linear superposition of these two eigenstates [12]. So far, several strategies have been reported for the dynamic manipulation of these OAM states, among which structured liquid crystals (LCs) [14,15] and metasurfaces [16,17] are the most commonly used. To improve the switching speed, polymer-stabilized blue phase LCs (BPLCs) driven by patterned electrodes [18], and cholesteric LCs with strong nonlinear effect [19] were introduced successively. Although the response time could be decreased to the scale of sub-millisecond and even picosecond, they suffer from ultra-high driving voltage or complicated facilities.

Ferroelectric liquid crystal (FLC) is another typical LC mesophase and well-known for its fast electro-optical response [20]. Compared with BPLCs and dual-frequency LCs, the switching speed of FLC can be one order faster, while the power consumption is still relatively

#380050 https://doi.org/10.1364/OE.27.036903
Journal © 2019 Received 10 Oct 2019; revised 19 Nov 2019; accepted 25 Nov 2019; published 4 Dec 2019

Optics EXPRESS

low. Unfortunately, the intrinsic diffraction is usually inevitable due to the periodic helical structure and ferroelectric domains of FLCs, restricting their applications in modern optics and photonics. To address this issue, an unique electro-optical mode, called electrically suppressed helix (ESH) mode, has been intensively studied since 2011 [21,22]. Depending on the polarity of the applied electric field, the molecules of ESH FLC rotate around the smectic helix and can be switched between two sides of the cone surface which are parallel to the substrates [20]. Low-voltage-driven fast response has been achieved conveniently [23,24]. Meanwhile, ESH FLC shows good alignment quality, and accordingly offers ultra-high optical contrast free from serious background diffraction [22,25,26]. Above features make such versatile LC material a promising candidate for the dynamic manipulation of OAM in a desirable way.

In this work, we combine the uniformly-aligned FLC with the space-variant photo-patterned nematic LC to realize the fast switching of OAM. Via just alternating the direction of the applied electric field, both the helicity of OAM and their superposed state (here, CVB) are actively switched in good beam quality, high efficiency and low power consumption. Particularly, even at a low voltage of 1.7 V/μm, the switching time is only 120 μs. It can be further decreased to enable a high-frequency over 6 kHz modulation of OAM with the increase of the driving voltage. This may extend the approach of fast-speed beam tailoring.

2. Principle

Two key optical elements of our strategy are the FLC wave-plate (FLC-WP) and the nematic LC q-plate. Here, the FLC material FD4004N (Dai-Nippon Ink and Chemicals, Japan) is adopted owing to its excellent properties of ESH mode [22]. Its phase transition scheme shows as SmC* → SmA → N* → Iso at 72 °C, 85 °C and 105 °C, respectively. At room temperature (*i.e.*, SmC* state), it has the spontaneous polarization $P_s \approx 61$ nC/cm^2 and the tilt angle $\theta \approx 22.05°$ [22].

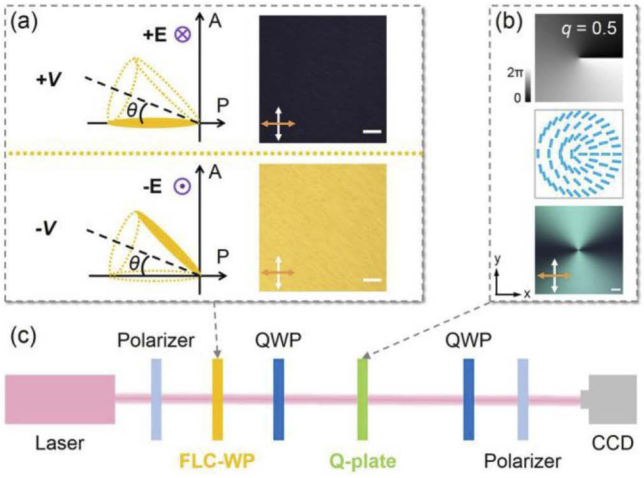

Fig. 1. (a) The schematic illustration of the FLC molecule orientation (yellow ellipse) under opposite electric field polarities, and respective micrographs recorded by a polarized optical microscope. θ is the tilt angle, *i.e.*, half of the cone angle of the FLC helical structure. The black dashed line indicates the alignment direction of FLC helix. Yellow double-ended arrow indicates the direction of polarizer (P), while white indicates analyzer (A). (b) The theoretical phase pattern, director distribution and experimental micrograph of a nematic LC q-plate with $q = 0.5$. All scale bars are 100 μm. (c) The optical setup to realize the fast switchable OAM. FLC-WP represents ferroelectric liquid crystal wave-plate, and QWP represents quarter-wave plate.

Optics EXPRESS

Without applying a voltage, the chirality of FD4004N induces a helical structure with the cone angle 2θ and a non-uniform texture is exhibited. While applying a perpendicular electric field over the critical value (typically ~ 0.5 V/μm), the helix will be completely suppressed and a uniform structure can be obtained. Determined by the polarity of the driving electric field, the LC directors orientate along two distinctive sides of the helical cone surface ($+\theta$ and $-\theta$) around the alignment direction, which are schematically illustrated in Fig. 1(a). Therefore, through homogenously aligning the FD4004N, a tunable wave-plate with the optical axis switching between 0° and $2\theta \approx 44.1°$ can be achieved. Notably, it is extremely close to the special angle 45°. Via controlling the FLC cell gap to be half-wave plate (HWP) or quarter-wave plate (QWP), it can alternate the incident linear or circular polarization states in a very high speed.

On the other hand, a nematic LC q-plate is introduced to generate the OAM beams. It is essentially an inhomogeneous wave-plate with the space-variant optical axis distribution following $\alpha = q\varphi + \alpha_0$, where q represents the variation frequency of the optical axis, φ is the azimuthal angle in the transverse x-y plane, α_0 is the initial orientation when $\varphi = 0$ and is usually assumed to be zero [27]. The theoretical phase pattern and the LC director distribution of an example with $q = 0.5$ are shown in Fig. 1(b). Q-plate is a typical geometric phase optical element and high-quality OVs/CVBs can be conveniently generated in high efficiency through the spin-to-OAM conversion [28]. Considering the sandwich configuration of a FLC-HWP, a conventional QWP and a q-plate, the incident linearly polarized light is transformed to

$$\begin{aligned}\mathbf{E}_{\text{out}} &= \mathbf{J}_q\mathbf{J}_{\text{QWP}}\mathbf{J}_{\text{FLC - HWP}}\mathbf{E}_{\text{in}} \\ &= \begin{bmatrix} \cos(2\alpha) & \sin(2\alpha) \\ \sin(2\alpha) & -\cos(2\alpha) \end{bmatrix}\begin{bmatrix} 1 & -i \\ -i & 1 \end{bmatrix}\begin{bmatrix} \cos(2\beta) & \sin(2\beta) \\ \sin(2\beta) & -\cos(2\beta) \end{bmatrix}\begin{bmatrix} 1 \\ 0 \end{bmatrix}\mathrm{E}_0, \\ &= \begin{bmatrix} \cos 2(\alpha-\beta) - i\sin 2(\alpha+\beta) \\ \sin 2(\alpha-\beta) + i\cos 2(\alpha+\beta) \end{bmatrix}\mathrm{E}_0\end{aligned} \tag{1}$$

where $\mathbf{J}_q$, $\mathbf{J}_{\text{QWP}}$ and $\mathbf{J}_{\text{FLC-HWP}}$ represent the Jones matrix [29] of the q-plate, QWP and FLC-HWP, respectively. β is the angle between the optical axis of the FLC-HWP and x-axis, which is electrically switched between 0° and 2θ. Approximately, two specific states can be obtained:

$$\mathbf{E}_{\text{out}} = \begin{cases} \mathrm{E}_0 e^{-i2q\varphi}\begin{bmatrix} 1 \\ +i \end{bmatrix}, \beta = 0° \\ -i\mathrm{E}_0 e^{i2q\varphi}\begin{bmatrix} 1 \\ -i \end{bmatrix}, \beta = 45° \end{cases}. \tag{2}$$

This indicates a fast and efficient switch between OVs carrying opposite topological charge ($m = -2q$ and $m = +2q$), *i.e.*, the OAM states with orthogonal helicity.

3. Experiment and results

To fabricate high-performance samples of the FLC-WP and q-plate, the photo-alignment technology is employed, which has been proved to be compatible with various kinds of LCs [30]. A polarization-sensitive azo-dye SD1 (Dai-Nippon Ink and Chemicals, Japan) was used as the photo-alignment agent, whose molecules tend to be perpendicular to the polarization direction of the illuminating UV light [31]. For the LC q-plate, a multi-step partly-overlapping exposure process [32] was performed to carry out the space-variant orientations, further verified by the continuously changing brightness of its micrograph shown in Fig. 1(b). For the uniformly-aligned FLC-WP, one indium-tin-oxide (ITO) substrate was spin-coated with the SD1 layer, irradiated by

Optics EXPRESS

a homogeneously polarized UV light and then assembled with another bare ITO substrate. The cell gap was maintained at 1.5 μm to secure the ESH mode characteristics and the half-wave condition for 632.8 nm. Figure 1(a) presents the micrographs of the fabricated FLC-HWP under opposite polarities of sufficiently high electric field. The typical ESH FLC textures with uniform domains are clearly observed. At the positive condition, the optical axis is parallel to the polarizer direction of the microscope. The incident light retains its polarization state after passing through the FLC cell, and then is blocked by the crossed analyzer, showing a dark state. While at the negative electric field, the optical axis is switched to be approximately 45° between the polarizer and analyzer. In this case, the incident polarization is rotated and a bright state is exhibited.

The optical setup to realize the fast switchable OAM is schematically exhibited in Fig. 1(c). The first polarizer, the FLC-WP and the former QWP are used to rapidly alternate the polarization state incident on the q-plate. Figure 2 shows the experimental results at the wavelength of 632.8 nm with the FLC-HWP under opposite voltages. When $V = +2.5$ V, $\beta = 0°$, and the incident light is right circularly polarized (RCP). Thus, the left circularly polarized (LCP) OV with topological charge $m = -1$ is generated as shown in Fig. 2(a). While at $V = -2.5$ V, $\beta = 44.1°$, and thus, the nearly RCP OV with $m = +1$ is obtained in Fig. 2(e). In order to verify the topological charge of the resultant OAM modes, the astigmatic transformation method [33] is adopted by inserting a cylindrical lens ($f = 100$ mm) in front of the CCD and capturing the converted pattern at its focal plane. The number of dark stripes and their tilt direction represent the value and sign of the topological charge. Detection results of OAM are revealed in Figs. 2(b) and 2(f), respectively. As expected, the number is same ($|m| = 1$) while the tilt is symmetric, confirming high-quality OAM states with orthogonal helicity.

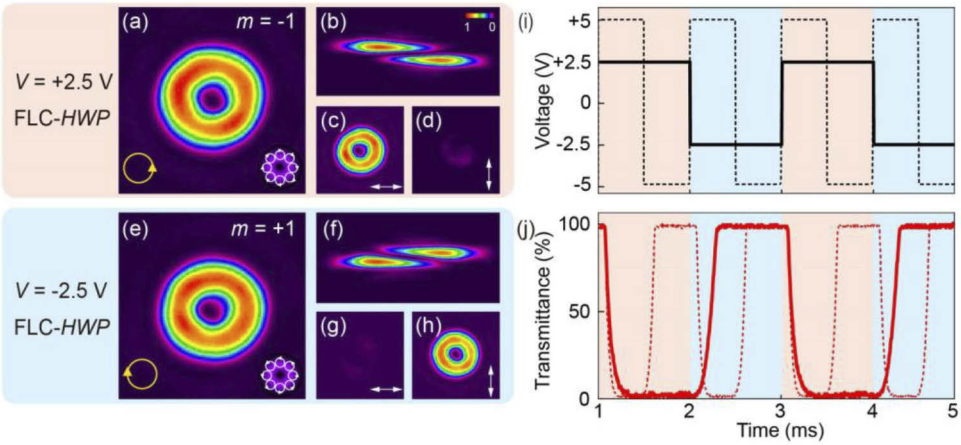

Fig. 2. Diffraction patterns at 632.8 nm with the applied voltage of FLC-HWP: (a) +2.5 V and (e) −2.5 V. Yellow circles represent the resultant incident polarization states (RCP and LCP) before illuminating the q-plate, and white circles indicate the generated OVs (LCP, $m = -1$, and RCP, $m = +1$). Corresponding OAM detection results based on the astigmatic transformation method are shown in (b) and (f), and the polarization measurements are shown in (c), (d) and (g), (h), respectively. White double-ended arrows represent the polarization direction of the second polarizer (*i.e.*, analyzer). The color bar indicates the relative optical intensity. (i) The waveform of the applied square wave to drive the FLC-WP: 5 V_{pp}, 500 Hz (solid line) and 10 V_{pp}, 1 kHz (dashed line). (j) The response curve of the OAM switching, where the polarization direction of the analyzer is set to be perpendicular to that of the polarizer. Solid and dashed lines correspond to the condition of 5 V_{pp} and 10 V_{pp}, respectively.

Optics EXPRESS

The combination of the latter QWP and the second polarizer (*i.e.*, analyzer) takes the role of output polarization detection. Corresponding measurement results shown in Figs. 2(c), 2(d) and 2(g), 2(h) verify their almost opposite circular polarization during the switching. Although there exists a little light leakage in dark states which could be attributed to the slight mismatch between 2θ and 45°, the contrast ratio still approaches 100, indicating a high conversion efficiency ~ 99% of the transmitted light. To quantitatively characterize the electro-optical performance, a square-wave electric field at the frequency of 500 Hz and the peak-to-peak voltage (V_{pp}) of 5 V is applied to drive the FLC-HWP, whose waveform is shown as the solid line in Fig. 2(i). With the polarization direction of the analyzer set to be perpendicular to that of the polarizer, a response curve of the OAM switching is obtained as depicted in Fig. 2(j). At such a low electric field of ~ 1.7 V/μm, the switching-on time, defined as the duration from 10% to 90% of the transmittance change, is measured as ~ 130 μs, while the switching-off time (90% to 10%) is ~ 120 μs. Increasing the driving voltage can further accelerate this symmetric switching process. Down to 75 μs is realized under 10 V_{pp}, which is experimentally verified as the dashed line in Fig. 2(j). Such a short response time enables the fast-speed modulation of OAM at a high frequency over 6 kHz.

The rapid alternation between orthogonal CVBs is also achievable based on this active FLC-HWP. Without the QWPs, the incident linear polarization either maintains horizontal, or is rotated around 90° to become vertical after passing through the FLC-HWP driven by positive or negative voltage, respectively. Accordingly, the CVB with polarization order $P = 2q = 1$ is generated, corresponding to the radial (Fig. 3(a)) and azimuthal (Fig. 3(c)) polarization state, which are the most typical types of superposed OAM states. After transmission through an analyzer, the lobe structures are either parallel (Fig. 3(b)) or perpendicular (Fig. 3(d)) to the orientation of the rotating analyzer, confirming their space-variant polarization distributions. The same excellent performance of fast response in low power consumption is acquired as well.

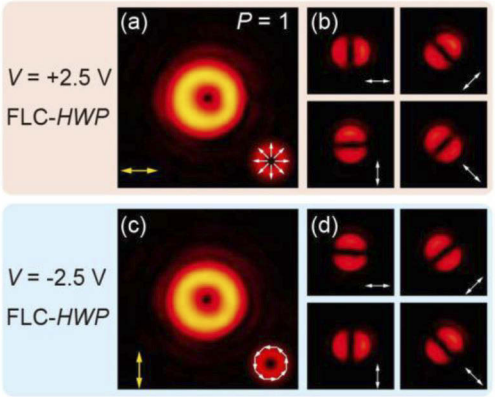

Fig. 3. Diffraction patterns at 632.8 nm without two QWPs under the applied voltage of FLC-HWP: (a) +2.5 V and (c) −2.5 V. The resultant incident polarization states (horizontal and vertical) of the *q*-plate are represented by the yellow arrows, and white arrows indicate the generated CVBs with $P = 1$ (radial and azimuthal). Corresponding polarization detections after transmission through a rotating analyzer labeled by white double-ended arrows are shown in (b) and (d), respectively.

In addition, another FLC-QWP for the wavelength of 520 nm is fabricated, enabling the fast dynamic conversion between OV and CVB, *i.e.*, single and superposed OAM state. At $V = +2.5$ V, the incident horizontal polarization results in the radial CVB (Fig. 4(a)), verified by the lobe structure of its polarization detection (Fig. 4(b)). After changing the polarity of the electric field, the FLC-QWP transforms the horizontal polarization to nearly RCP. An OV with LCP

Optics EXPRESS

and $m = -1$ is acquired as shown in Fig. 4(e), which remains a ring intensity pattern with just a decreased intensity after the analyzer (Fig. 4(f)). Another example with larger topological charge is also demonstrated in Figs. 4(c), 4(d), and 4(g), 4(h). Diffraction pattern featuring six lobes is obtained for the polarization measurement of such superposed OAM state. Here only some special cases of OVs and CVBs are presented. In fact, this method could be further extended to the fast switch between any two different points on the higher-order Poincaré sphere.

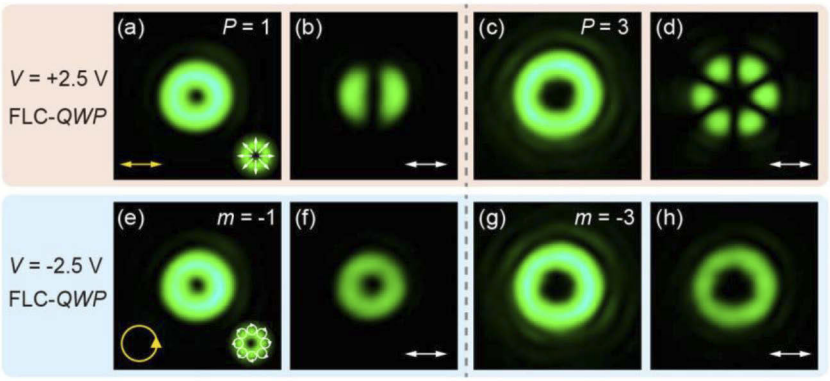

Fig. 4. Diffraction patterns at 520 nm without two QWPs under the applied voltage of FLC-QWP: (a) +2.5 V and (e) −2.5 V. The resultant incident polarization states (horizontal and RCP) of the q-plate with $q = 0.5$ are represented by the yellow arrows, and white arrows indicate the generated CVB with $P = 1$ radial polarization and OV with LCP $m = -1$. Corresponding polarization detections after transmission through the analyzer labeled by white double-ended arrows are shown in (b) and (f), respectively. For the q-plate with $q = 1.5$, experimental results are shown in (c), (d), and (g), (h), respectively.

4. Conclusions

In summary, we proposed an approach for the fast switchable OAM of light. By means of the uniform FLC-WP and the space-variant patterned LC q-plate, the rapid and efficient conversion between different OAM beams, possessing opposite helicity and orthogonal spatial-mode states, has been demonstrated in high quality and good electrical controllability. The response time can reach 75 μs with a low voltage of ± 5 V, making high-frequency manipulation of OAM possible. Corresponding performance could be further improved with the proper design of chiral compound for optimized spontaneous polarization and rotational viscosity of FLC materials. This work provides more possibilities towards the research of ultra-fast tailoring of arbitrary structured beams, not limited to OAM, and may facilitate numerous cutting-edge applications from optical trapping, optical communications, to quantum informatics.

Funding

National Key Research and Development Program of China (2017YFA0303700); National Natural Science Foundation of China (61435008, 61490714, 61575093, 61875004, 61922038); ; Distinguished Young Scholars Fund of Jiangsu Province (BK20180004); Fundamental Research Funds for the Central Universities (021014380118).

Disclosures

The authors declare no conflicts of interest.

Optics EXPRESS

References

1. L. Allen, M. W. Beijersbergen, R. J. C. Spreeuw, and J. P. Woerdman, "Orbital angular-momentun of light and the laguerre-gaussian laser modes," Phys. Rev. A **45**(11), 8185–8189 (1992).
2. A. M. Yao and M. J. Padgett, "Orbital angular momentum: origins, behavior and applications," Adv. Opt. Photonics **3**(2), 161–204 (2011).
3. M. Woerdemann, C. Alpmann, M. Esseling, and C. Denz, "Advanced optical trapping by complex beam shaping," Laser Photonics Rev. **7**(6), 839–854 (2013).
4. M. Padgett and R. Bowman, "Tweezers with a twist," Nat. Photonics **5**(6), 343–348 (2011).
5. J. Wang, J. Y. Yang, I. M. Fazal, N. Ahmed, Y. Yan, H. Huang, Y. Ren, Y. Yue, S. Dolinar, M. Tur, and A. E. Willner, "Terabit free-space data transmission employing orbital angular momentum multiplexing," Nat. Photonics **6**(7), 488–496 (2012).
6. A. E. Willner, H. Huang, Y. Yan, Y. Ren, N. Ahmed, G. Xie, C. Bao, L. Li, Y. Cao, Z. Zhao, J. Wang, M. P. J. Lavery, M. Tur, S. Ramachandran, A. F. Molisch, N. Ashrafi, and S. Ashrafi, "Optical communications using orbital angular momentum beams," Adv. Opt. Photonics **7**(1), 66–106 (2015).
7. K. Toyoda, F. Takahashi, S. Takizawa, Y. Tokizane, K. Miyamoto, R. Morita, and T. Omatsu, "Transfer of light helicity to nanostructures," Phys. Rev. Lett. **110**(14), 143603 (2013).
8. J. Ni, C. Wang, C. Zhang, Y. Hu, L. Yang, Z. Lao, B. Xu, J. Li, D. Wu, and J. Chu, "Three-dimensional chiral microstructures fabricated by structured optical vortices in isotropic material," Light: Sci. Appl. **6**(7), e17011 (2017).
9. J. H. Lee, G. Foo, E. G. Johnson, and G. A. Swartzlander Jr, "Experimental verification of an optical vortex coronagraph," Phys. Rev. Lett. **97**(5), 053901 (2006).
10. A. Aleksanyan, N. Kravets, and E. Brasselet, "Multiple-star system adaptive vortex coronagraphy using a liquid crystal light valve," Phys. Rev. Lett. **118**(20), 203902 (2017).
11. Q. Zhan, "Cylindrical vector beams: from mathematical concepts to applications," Adv. Opt. Photonics **1**(1), 1–57 (2009).
12. G. Milione, H. Sztul, D. Nolan, and R. Alfano, "Higher-order Poincaré sphere, Stokes parameters, and the angular momentum of light," Phys. Rev. Lett. **107**(5), 053601 (2011).
13. P. Chen, S. J. Ge, W. Duan, B. Y. Wei, G. X. Cui, W. Hu, and Y. Q. Lu, "Digitalized geometric phases for parallel optical spin and orbital angular momentum encoding," ACS Photonics **4**(6), 1333–1338 (2017).
14. R. Barboza, U. Bortolozzo, M. Clerc, S. Residori, and E. Vidal-Henriquez, "Optical vortex induction via light–matter interaction in liquid-crystal media," Adv. Opt. Photonics **7**(3), 635–683 (2015).
15. P. Chen, B. Y. Wei, W. Hu, and Y. Q. Lu, "Liquid-crystal-mediated geometric phase: from transmissive to broadband reflective planar optics," Adv. Mater. **31**, 1903665 (2019).
16. N. Yu and F. Capasso, "Flat optics with designer metasurfaces," Nat. Mater. **13**(2), 139–150 (2014).
17. P. Yu, J. Li, X. Li, G. Schütz, M. Hirscher, S. Zhang, and N. Liu, "Generation of switchable singular beams with dynamic metasurfaces," ACS Nano **13**(6), 7100–7106 (2019).
18. S. J. Ge, P. Chen, L. L. Ma, Z. Liu, Z. G. Zheng, D. Shen, W. Hu, and Y. Q. Lu, "Optical array generator based on blue phase liquid crystal Dammann grating," Opt. Mater. Express **6**(4), 1087–1092 (2016).
19. Y. Liu, H. Liang, C. W. Chen, X. Xie, W. Hu, P. Chen, J. Wen, J. Zhou, T. H. Lin, and I. C. Khoo, "Ultrafast switching of optical singularity eigenstates with compact integrable liquid crystal structures," Opt. Express **26**(22), 28818–28826 (2018).
20. A. K. Srivastava, V. G. Chigrinov, and H. S. Kwok, "Ferroelectric liquid crystals: excellent tool for modern displays and photonics," J. Soc. Inf. Disp. **23**(6), 253–272 (2015).
21. E. Pozhidaev, V. G. Chigrinov, V. Vashchenko, M. Minchenko, A. Srivastava, V. Molkin, A. Krivoshey, S. Torgova, and H. Kwok, "High frequency low voltage shock-free ferroelectric liquid crystal: a new electro- optical mode with electrically suppressed helix," in *Proceedings of the 31th International Display Research Conference EuroDisplay* (2011).
22. A. K. Srivastava, W. Hu, V. G. Chigrinov, A. D. Kiselev, and Y. Q. Lu, "Fast switchable grating based on orthogonal photo alignments of ferroelectric liquid crystals," Appl. Phys. Lett. **101**(3), 031112 (2012).
23. A. K. Srivastava, X. Q. Wang, S. Q. Gong, D. Shen, Y. Q. Lu, V. G. Chigrinov, and H. S. Kwok, "Micro-patterned photo-aligned ferroelectric liquid crystal Fresnel zone lens," Opt. Lett. **40**(8), 1643–1646 (2015).
24. Q. Guo, L. Xu, J. Sun, X. Yang, H. Liu, K. Yan, H. Zhao, V. G. Chigrinov, and H. S. Kwok, "Fast switching beam steering based on ferroelectric liquid crystal phase shutter and polarisation grating," Liq. Cryst. **46**(9), 1383–1388 (2019).
25. Y. Ma, B. Y. Wei, L. Y. Shi, A. K. Srivastava, V. G. Chigrinov, H. S. Kwok, W. Hu, and Y. Q. Lu, "Fork gratings based on ferroelectric liquid crystals," Opt. Express **24**(6), 5822–5828 (2016).
26. F. Fan, L. Yao, X. Wang, L. Shi, A. K. Srivastava, V. G. Chigrinov, H. S. Kwok, and S. C. Wen, "Ferroelectric liquid crystal dammann grating by patterned photoalignment," Crystals **7**(3), 79 (2017).
27. L. Marrucci, C. Manzo, and D. Paparo, "Optical spin-to-orbital angular momentum conversion in inhomogeneous anisotropic media," Phys. Rev. Lett. **96**(16), 163905 (2006).
28. F. Cardano, E. Karimi, S. Slussarenko, L. Marrucci, C. de Lisio, and E. Santamato, "Polarization pattern of vector vortex beams generated by q-plates with different topological charges," Appl. Opt. **51**(10), C1–C6 (2012).
29. P. Yeh and C. Gu, *Optics of Liquid Crystal Displays* (John Wiley & Sons, 1999).

Optics EXPRESS

30. V. G. Chigrinov, V. M. Kozenkov, and H. S. Kwok, *Photoalignment of Liquid Crystalline Materials: Physics and Applications* (John Wiley & Sons, 2008).
31. V. Chigrinov, S. Pikin, A. Verevochnikov, V. Kozenkov, M. Khazimullin, J. Ho, D. D. Huang, and H. S. Kwok, "Diffusion model of photoaligning in azo-dye layers," Phys. Rev. E **69**(6), 061713 (2004).
32. P. Chen, L. L. Ma, W. Hu, Z. X. Shen, H. K. Bisoyi, S. B. Wu, S. J. Ge, Q. Li, and Y. Q. Lu, "Chirality invertible superstructure mediated active planar optics," Nat. Commun. **10**(1), 2518 (2019).
33. V. Denisenko, V. Shvedov, A. S. Desyatnikov, D. N. Neshev, W. Krolikowski, A. Volyar, M. Soskin, and Y. S. Kivshar, "Determination of topological charges of polychromatic optical vortices," Opt. Express **17**(26), 23374–23379 (2009).